NEW METHODS FOR IMPROVED AND ACCELERATED FE-VOLUME CONDUCTOR MODELLING IN EEG/MEG-SOURCE RECONSTRUCTION

C.H.Wolters[1], U.Hartmann[2], M.Koch[3], F.Kruggel[4], S.Burkhardt[5], A.Basermann[6], D.S.Tuch[7] and J.Haueisen[8]

1. ABSTRACT

Localising the current distribution in the human brain from extracranial EEG/MEG-measurements is an Inverse Problem whose solution requires the repeated simulation of the electric/magnetic propagation for a given dipolar source in the brain using a volume-conduction head model. The simulations are referred to as the Forward Problem. In order to model the head most realistically, the different head tissues first have to be segmented and then assigned individual conductivity tensor material parameters. The T_1-MRI-based CSF–skull boundary identification is problematic. In this paper we present techniques for an improved skull segmentation by means of multi-MR-imaging protocol registration and segmentation strategies. Recently, a formalism has been described for relating the effective electrical conductivity tensor of white matter tissue to the effective water diffusion tensor as measured by diffusion MRI, the DTI-EMA. Whole-head diffusion tensor data have been acquired in order to improve white matter modelling in future investigations. The use of fast techniques to solve the linear equation systems arising from the 3-D finite element method is necessary with regard to an appropriate solution time for high resolution models and inverse source localisation. This paper compares different iterative strategies for sparse linear equation systems and their parallelisation.

Keywords: EEG/MEG source localisation, Finite element method, Multi-MR-imaging protocol-based skull segmentation, DTI-EMA, Fast parallelised solver techniques

---

[1]Ph.D. student and Research Staff Member, MEG group, MPI of Cognitive Neuroscience in cooperation with the MPI for Mathematics in the Sciences, Muldentalweg 9, 04828 Bennewitz, Germany
[2] Dr., Research Staff Member, NEC Europe C&C Research Laboratories, 53757 St.Augustin, Germany
[3] Ph.D. student, NMR group, MPI of Cognitive Neuroscience, Stephanstr.1a, 04103 Leipzig, Germany
[4] Dr. , Head of the SIP group, MPI of Cognitive Neuroscience, Stephanstr.1a, 04103 Leipzig, Germany
[5] Student assistant, MPI for Mathematics in the Sciences, Inselstr.22-26, 04103 Leipzig, Germany
[6] Dr., Research Staff Member, NEC Europe C&C Research Laboratories, 53757 St.Augustin, Germany
[7] Ph.D.student, MGH-NMR center, Bldg.149, 13th St., Charlestown, MA 02129, USA
[8] Dr., Head of the Biomag. Center, F.-Schiller-University Jena, Philosophenweg 3, 07740 Jena, Germany

2. INTRODUCTION

It is normal practice in cognitive research and in clinical routine and research to localise dipolar primary current sources in the human brain. Examples are the study of functional cortical organisation in epilepsy and cognition by means of measured (evoked) Electroencephalography (EEG) and/or Magnetoencephalography (MEG). The primary sources $\vec{j}_p$ are electrolytic currents within the dendrites of the large pyramidal cells of activated neurons. Under knowledge of the head tissue conductivities σ, the electric potential ϕ arising from a known $\vec{j}_p$ can be described by means of the quasistatic approach of Maxwell's equations of electrodynamics

$$\begin{aligned} \nabla \cdot (\sigma \nabla \phi) &= \nabla \cdot \vec{j}_p \qquad in\ \Omega \\ \sigma \left. \frac{\partial \phi}{\partial \vec{n}} \right|_{\Gamma_{scalp}} &= 0 \\ \phi_{ref} &= 0. \end{aligned} \tag{1}$$

In this formula, Γ_{scalp} is the surface of the head Ω and ϕ_{ref} the potential at the reference electrode. The magnetic flux Φ through an MEG-magnetometer L can then be calculated using a corollary from Biot-Savart's law:

$$\Phi = \frac{-\mu}{4\pi} \oint_L \iiint_\Omega \frac{\vec{j}_p(\vec{x}) + \sigma(\vec{x}) \nabla \phi(\vec{x})}{\left\| \vec{x} - \vec{l} \right\|} d\vec{x} d\vec{l} \ . \tag{2}$$

μ in this formula is the magnetic permeability of the vacuum. Seen from the view of numerical optimisation, the Inverse Problem is a minimisation problem, in which the calculation of the difference between EEG/MEG measurements and a particular forward solution (data term) plus a source regularisation (model term) is an objective function evaluation (1, 2).

Today's commercially available source-reconstruction tools model the head as a realistically shaped three-layer-model with constant and isotropic conductivity (IC) on each of the layers skin, skull and brain. Under these assumptions the differential equation (1) can be transformed into an integral equation which can be solved by means of the boundary element method (Fig.1). The arising linear equation system used in practise has about 4000 unknowns and a full and asymmetrical geometry matrix. After inverting this matrix once, the solution for every primary source needs one matrix-vector operation (4000^2 mult., not taking into account the numerically important isolated problem approach). A second technique of volume conductor modelling is offered by the 3D-finite element method (Fig.2), which numerically solves equation (1) in the variational formulation. This method is able to treat geometries of arbitrary complexity and inhomogeneous and anisotropic conductivity material properties. Nevertheless, most of the *in vivo* conductivity measurements found in the literature were conducted 30 years ago and the values obtained vary over a wide range. They differ not only between *in vivo* and *in vitro* measurements, but also depend on age, state of health, environmental factors, and personal constitution (see overview in 3). A strongly anisotropic conductivity (AC) with a ratio of 1:9 (normal:parallel to fibers) has been measured for brain white matter. If the whole skull, from a more macroscopic point of view, is regarded as one unit consisting

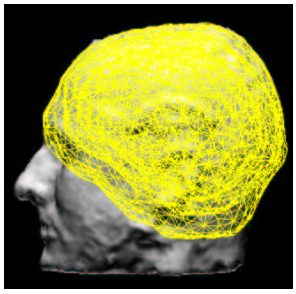

Fig.1: BE-Model (1500 nodes).

of a soft bone layer enclosed by two hard bone layers, its conductivity shows a comparable anisotropy (radially: tangentially to the skull surface). In the latter case, the principal directions of the conductivity tensor for every finite element can be determined from the segmented skull surface making modelling much simpler than for white matter. To summarise: Methods are needed that can give the best possible estimates of the individual conductivity parameters inside the human head. This should hopefully also lead to better standard models for quantitative cognitive research. In today's science two such methods are under investigation: Electrical Impedance Tomography (EIT) (4) and the Diffusion Tensor Imaging Effective Medium Approach (DTI-EMA) (5). Our study will use high resolution FE-techniques, multi-MR-image protocols for skull segmentation, and DTI-EMA for a more realistic white matter modelling to improve the volume conductor model.

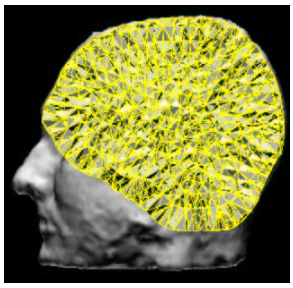

Fig2: FE-Model

3.METHODS

A prerequisite for an appropriate modelling of the volume conductor is the segmentation of head tissues with different resistivity properties. It has been shown that the modelling of the inhomogeneous (6) and anisotropic (7) low-conducting properties of the human skull is of special importance for EEG/MEG-source localisation. The identification of the cerebrospinal fluid(CSF)–skull boundary based on T_1-weighted MRI (T_1-MRI) is problematic, and Proton-Density-Weighting (PD-MRI) is most suitable for this task. To exploit both MR-imaging protocols, the PD-MRI has to be registered onto the T_1-MRI. We examined two registration techniques: a linear non-rigid edge registration of the pre-segmented outer skull surfaces on both image protocols using genetic optimisation (8) and a voxel-similarity based rigid registration without any pre-segmentation using a cost function based on mutual information and an optimisation by means of Powell's direction set method (9). Segmentation of ventricles, white matter, grey matter, skull and scalp-tissues was then carried out using the toolkit BRIAN (10).

Basser et al. (11) introduced the assumption that the effective electrical conductivity tensor shares the eigenvectors with the effective diffusion tensor of water, which can be measured for white matter tissue by DTI-MRI. A linear relationship between the eigenvalues of both tensors for small intracellular diffusion and high resistivity of the cell membrane was proposed by Tuch et al. (5). Their proposition is based on a self-consistent differential effective medium approach (EMA) for the dielectric constant (for low frequencies the conductivity) of porous media, derived from a multiple scattering formula from solid state physics developed by Sen et al.(12). Latour et al. (13) derived a similar EMA for the effective water diffusion in biological cells. The coupling of both EMA-formulae through the unknown porosity variable led to the linear dependence of the eigenvalues described in (5).

A geometry-based (1) and a voxel-based (14) mesh generator were coupled to the finite element tool CAUCHY (1,2). Several parallel linear equation solvers were implemented on the NEC Cenju-4 supercomputer whose 64 processors (MIPS R10000) are arranged in a multi stage interconnection network (15,16). The Quasi-Minimum-Residual (QMR) method for symmetric matrices is diagonally preconditioned and requires only one matrix-vector multiplication per iteration. The BI-CGSTAB algorithm exploits Incomplete LU preconditioning with Threshold (10^{-2}) (ILUT). The effect of the Reverse Cuthill-McKee (RCM) matrix ordering for reducing the bandwidth was also investigated.

4.RESULTS

Magnetic resonance imaging was performed on a 3 Tesla whole-body scanner (Medspec 30/100, Bruker, Ettlingen/Germany). The 3D T_1-MRI was acquired using an inversion recovery MDEFT (17) sequence. For the PD-MRI a 3D FLASH (18) protocol was employed. The resolution was $1\times1\times1.5mm^3$ in both acquisitions. Fig.3 shows the registration result of the PD-MRI onto the T_1-MRI using the voxel-similarity based rigid registration method (middle) and the 6-tissue-segmentation exploiting the edge-registration method (right).

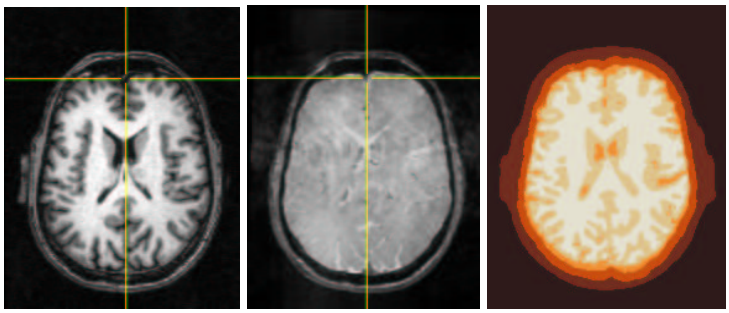

Fig.3: T_1-MRI (left), voxel-registered PD-MRI (middle), segmentation result exploiting edge registration (right).

Whole-head-DTI was performed using a 4-slice displaced U-FLARE (19) protocol with centric phase-encoding. Diffusion weighting was implemented as a Stejskal-Tanner type spin-echo preparation. Although echo planar imaging (EPI) is being widely applied for DTI purposes, U-FLARE was preferred to EPI in order to avoid spatial misregistration between the DTI data and the 3D data sets due to magnetic field inhomogeneities. The effective echo time was T_{eff} = 120 ms, and TR = 11 s. The diffusion weighting gradient pulses had a duration of 22 ms, and their onset was separated by 40 ms. Four different *b* values evenly spaced between 50 and 800 s/mm^2 were applied through variation of the gradient strength. The slices were axially oriented and 5 mm thick. In-plane resolution was 2×2 mm^2. In order to increase the signal-to-noise ratio, 5 to 16 images (depending on the *b* value) with identical diffusion weighting were averaged. Due to the long measurement time (50 min for 4 slices) data acquisition was split into 8 sessions. Coregistered T_1-MDEFT images of the same slices allow registration of the DTI data on the 3D data sets. Diffusion tensor calculation (20) was based on a multivariate regression algorithm in IDL (Interactive Data Language, Research Scientific, Bolder, Colorado/USA). Fig.4 shows a colour-coded map of the direction with the largest principal diffusivity (green = horizontal, red = vertical, blue = through-plane), overlaid upon a T_1 image. Colouring in regions of low diffusion anisotropy was suppressed. The image correctly reproduces the white matter fibre directions and the relative isotropy of grey matter and CSF.

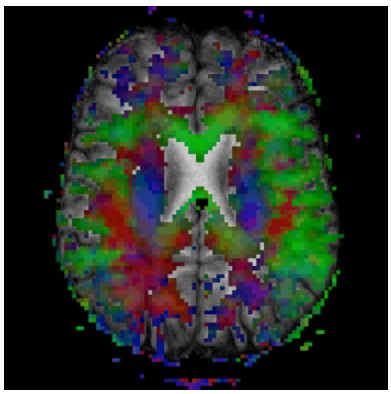

Fig.4: DTI-MRI

A four-layer spherical test volume conductor with constant and isotropic conductivity values on every layer was constructed and a 4mm isotropic cube mesh was generated using the voxel-based mesh generator. The symmetric geometry matrix

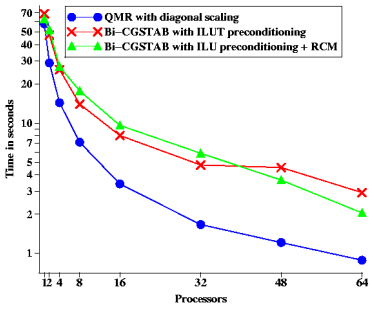

Fig.5: Solver Performance

corresponding to this test mesh - with an order of 71,403 and 1.402,157 non-zero entries - was set up with CAUCHY. A radially oriented primary source was placed in the inner sphere and the equation system was solved with the three proposed solution techniques. The execution times depending on the number of processors are depicted in Fig.5.

5.DISCUSSION

The important segmentation of the low conducting skull has been solved by registering a PD-MRI onto the corresponding T_1-MRI. If just a T_1-image is used, the inner skull surface can only be approximated by smoothing and dilating the segmented brain surface (1). Nevertheless, MR-image protocols contain nonlinear distortions and these are not identical for different protocols. In future studies, we will examine algorithms to correct for the relative nonlinear distortion differences between different protocols. Further studies will be carried out to examine the sensitivity of source reconstructions (focal and distributed sources, and diverse locations, orientations, and depths in the brain) to segmentation and AC of the skull and to white matter AC. The white matter AC will be calculated by means of DTI-EMA using the presented whole-head diffusion measurements. Preliminary results concerning the influence of white matter AC on the EEG/MEG forward solution for focal sources in different depths (21) encourage us to systematically study the extent of the inverse mislocalisation caused by the simplified white-matter modelling. A further goal is the validation of the DTI-EMA with a rabbit study using implanted physical sources.
In order to be able to apply high resolution FE-modelling for the inverse current reconstruction, efficient parallelised sparse matrix solvers are indispensable. The diagonally preconditioned QMR method for symmetric matrices showed the best time and scaling behaviour of the three techniques compared. In fact, on 64 processors the QMR speedup is slightly superlinear (i.e., 65) due to cache effects. The solvers tested within this paper are most appropriate for high-resolution forward modelling with great demand for memory or for forward modelling with a moderate number of dipoles (e.g., functional MRI-constrained source reconstructions exploiting the high temporal resolution of EEG/MEG). However, in most studies the forward solution has to be calculated for many different sources during the inverse optimisation procedures. Therefore parallelisation on the dipole level (every processor calculates a solution for one dipole to assemble the lead field matrix) (22) is most efficient, but only practicable if the demand for memory is not beyond the available resources. In future investigations we will couple iterative solvers and dipole level parallelisation with the efficient preconditioning of the Incomplete Cholesky Factorisation with Threshold (ICCT) or of Sparse Approximate Inverse techniques, which can be tuned for a maximal exploitation of the available memory resources and a minimal demand for subsequent iterations after preconditioning.

6.REFERENCES

1. Buchner, H., Knoll, G., Fuchs, M., Rienäcker, A., Beckmann, R., Wagner, M., Silny, J. and Pesch, J., Inverse localisation of electric dipole current sources in finite element models of the human head, Electroenc. Clin. Neurophysiol., 1997, Vol.102, 267-278.
2. Wolters, C.H., Beckmann, R.F., Rienäcker, A. and Buchner, H., Comparing regularised and non-regularised nonlinear dipole fit methods: A study in a simulated sulcus structure, Brain Topography, 1999, Vol.12 (1), 3-18.
3. Haueisen, J., Methods of numerical field calculation for neuromagnetic source

localisation, Dissertation, ISBN 3-8265-1691-5, Shaker Verlag Gmbh, Aachen.
4. Vauhkonen, P.J., Vauhkonen, M., Savolainen, T. and Kaipio, J.P., Static 3D electrical impedance tomography, Annals N. Y. Acad.Sci., 1999,Vol.873, 472-481.
5. Tuch, D.S., Wedeen, V.J., Dale, A.M. and Belliveau, J.W., Electrical conductivity tensor map of the human brain using NMR diffusion imaging: An effective medium approach, ISMRM, 6th Scientific Meeting, Sydney, 1998.
6. Pohlmeier, R., Buchner, H. and Knoll, G., The influence of skull-conductivity misspecification on inverse source localisation in realistically shaped finite element head models, Brain Topography, 1997, 9(3), 157-162.
7. Marin, G. Guerin, C., Baillet, S., Garnero, L. and Meunier, G., Influence of skull anisotropy for the forward and inverse problem in EEG: Simulation studies using the FEM on realistic head models, Human Brain Mapping, 1998, 6, 250-269.
8. Staib, L.H. and Lei, X., Intermodality 3D medical image registration with global search, IEEE Workshop on Biomedical Image Analysis, Seattle, June 1994, pp.225-234, IEEE Computer Society Press, Los Alamitos.
9. Maes, F., Collignon, A., Vandermeulen, D., Marchal, G. and Suetens, P., Multimodality image registration by maximisation of mutual information, IEEE Transactions on Medical Imaging, 1997, Vol. 16 (2), 187-198.
10. Kruggel, F. and Lohmann, G., BRIAN-A toolkit for the analysis of multimodal brain datasets. In H.U.Lemke, K.Inamura, C.C.Jaffe, M.W.Vannier (eds.), Proceedings of the Computer Aided Radiology 1996 (CAR'96), Paris, pp. 323-328, Berlin, Springer.
11. Basser, P.J., Mattiello, J. and Bihan, D., MR diffusion tensor spectroscopy and imaging, Biophysical Journal, 1994, Vol.66, 259-267.
12. Sen, P.N., Scala, C. and Cohen, M.H., A self-similar model for sed. rocks with appl. to the dielectric constant of fused glass beads, Geophysics, 1981, Vol.46 (5), 781-795.
13. Latour, L.L., Svoboda, K., Mitra, P.P. and Sotak, C.H., Time-dependent diffusion of water in a biological model system, Proc.Natl.Acad.Sci.USA, 1994, Vol.91, 1229-1233.
14. Hartmann, U. and Kruggel, F., Transient analysis of the biomechanics of the human head with a high-resolution 3D finite element model, Computer Methods in Biomechanics and Biomedical Engineering, 1998, 2 (1), 49-64.
15. Basermann, A., Parallel block ILUT precond. for sparse eigenprob. and sparse linear systems, Proc. of the Int. Conference on Preconditioning Techniques for Large Sparse Matrix Problems in Industrial Applications (Sparse99), 1999, Minneapolis, 233-239.
16. Saad, Y., Iterative methods for sparse lin. sys., PWS Publ. Comp., Boston, 1996.
17. Lee, J.-H., Garwood, M., Menon, R., Adriany, G., Anderson, P., Truwit, C.L., and Ugurbil, K., High Contrast and Fast Three-Dim. Magnetic Resonance Imaging at High Fields, Magn. Reson. Med., 1995, Vol.34, 308-312.
18. Haase, A., Frahm, J., Matthaei, D., Hänicke, W., Merboldt, K.-D., FLASH imag.: rapid NMR imag. using low flip-angle pulses, J. Magn. Reson., 1986, Vol.67, 258-266.
19. Norris, D.G., Börnert, P., Coherence and interference in ultra-fast RARE experiments, J. Magn. Reson. A 105, 1993, 123-127.
20. Basser, P.J., Mattiello, J., LeBihan, D., Estimation of the effective self-diffusion tensor from the NMR spin echo, J. Magn. Reson. B 103, 1994, 247-254.
21. Haueisen, J., Tuch, D.S., Ramon, C., Schimpf, P. and Nowak, H., Conductivity tensor information in a 3-D finite element model of the human head for MEG and EEG forward computations, NeuroImage, Vol.10, Nr.3, September 1999, 4th International Hans Berger Conference, September 26-29, 1999.
22. Buchner, H., Darvas, F., Friedrich, V., Fuchs,M., Knepper,A., Knoll, G., Meyer-Ebrecht, D., Rienäcker, A., Sloot, P.M.A. and Waßmuth, K., Localisation of the electromag. activity of the brain in its indiv. anat., Fut. Gen. Comp. Syst., in press.